Edelweiss Applied Science and Technology
ISSN: 2576-8484
Vol. 10, No. 4, 112-124
2026
Publisher: Learning Gate
DOI: 10.55214/2576-8484.v10i4.12562

Equal swept-area experimental comparison of savonius and H-type darrieus vertical axis wind turbines for floating net cages microloads

Herlina Herlina[1*], Tajuddin Nur[2], Dewi Puspitasari[3], Syarifa Fitria[4]
[1,3,4]Department of Electrical Engineering, Universitas Sriwijaya, Inderalaya, South Sumatera, 30862, Indonesia; herlinawahab@unsri.ac.id (H.H.) dewipuspitasari@unsri.ac.id (D.P.) Syarifafitria@ft.unsri.ac.id (S.F.).
[2]Department of Electrical Engineering, Atma Jaya Catholic University of Indonesia, Jakarta, 12930, Indonesia; tans@atmajaya.ac.id (T.N.).

Abstract: Floating net cages (FNCs) in coastal aquaculture require a reliable, low-power electricity supply for daily operations. However, many coastal sites still have limited grid access and depend on fuel-based energy. This study compared the performance of a Savonius rotor and an H-type Darrieus rotor as renewable electricity options for FNC applications, using the same swept area of 0.45 m² and a shared direct-current generator interface under controlled laboratory airflow. A total of 560 operating points were recorded at wind speeds of 1.5–8.0 m/s under discrete resistive loads. Electrical power generation was derived from the measured voltage and current, while the wind-to-electric efficiency was determined as the proportion of generated electrical power to the available wind power. The findings indicated that the H-type Darrieus turbine exhibited superior performance compared to the Savonius turbine across the entire testing range. Its mean electrical power reached 7.59 W, compared with 4.47 W for the Savonius, while mean efficiency reached 17.01% and 10.09%, respectively. At 8.0 m/s, the H-type Darrieus produced 22.01 W, whereas the Savonius produced 12.47 W. These results indicate that the H-type Darrieus rotor is more suitable for the early-stage design of hybrid wind-solar-battery systems for FNC applications.

Keywords: *Floating net cages, H-type Darrieus rotor, Multivariate analysis, Savonius rotor, Vertical axis wind turbine, Wind-to-electric efficiency.*

1. Introduction

Coastal aquaculture increasingly depends on electricity for aeration, pumping, feeding, lighting, and routine water-quality management, and energy demand rises as farms intensify production and extend operating hours [1-3]. Energy consumption and associated greenhouse-gas emissions, therefore, remain key sustainability constraints across many aquaculture supply chains, especially where farms rely on fossil-based electricity or on-site engines [4, 5]. Many floating net cage (FNC) sites still operate with weak grid access, unstable voltage, or expensive diesel backup, so operators need reliable micro-scale power sources that can lower operating costs while reducing emissions [6-8]. Recent designs for aquaculture-oriented hybrid energy systems explicitly target oxygenation and other time-critical microloads, so system reliability and storage strategy matter as much as average annual energy yield [9, 10].

Solar photovoltaics already support aquaculture operations, but floating or fishery-complementary installations can change near-surface meteorology, evaporation, and water-quality indicators through shading and altered heat exchange [11, 12]. Systematic reviews and bibliometric evidence also show rapid growth of aquavoltaics research and highlight trade-offs among energy yield, ecosystem response, and operational constraints in aquaculture ponds and coastal sites [13, 14]. Whole-waterbody observations and recent syntheses report measurable impacts of floating photovoltaic coverage on light

History: Received: 29 January 2025; Revised: 5 March 2026; Accepted: 10 March 2026; Published: 30 March 2026
* Correspondence: herlinawahab@unsri.ac.id

availability, thermal structure, oxygen dynamics, and biodiversity, which make site-specific environmental safeguards part of effective energy design [15-17]. At the same time, technical reviews emphasize that float design, anchoring, and biofouling management often dominate reliability and lifecycle costs for floating photovoltaic deployments in practice [18].

Photovoltaic output drops at night and during extended cloud cover, so hybrid configurations that combine photovoltaics with wind and storage remain a practical pathway for continuous microloads in aquaculture operations [19]. Recent optimization studies show that load-profile resolution and storage-control assumptions can materially shift optimal sizing and economics, and choices for modeling battery performance can change design decisions in both grid-connected and islanded contexts [20-22].

Vertical axis wind turbines (VAWTs) are suitable for compact and near-load deployments because they accept changing wind directions without a yaw system and can operate in turbulent, non-uniform inflow common around coastal structures and aquaculture facilities [23, 24]. Accordingly, recent VAWT research targets low-to-medium wind regimes through flow-control devices, concentrator concepts, and rotor-arrangement strategies that aim to increase useful torque while keeping mechanical layouts simple [25, 26]. From a rotor-selection perspective, Savonius turbines offer strong self-starting behavior and tolerance to turbulence, whereas H-type Darrieus turbines typically deliver higher conversion efficiency but may face low-speed torque limitations that motivate aerodynamic and material design improvements [27]. Recent Energy Conversion and Management studies also show that rotor staging and rotor-to-rotor interaction designs can lift Savonius performance, which reinforces the need for controlled, like-for-like electrical comparisons when selecting small VAWTs for microload supply [28, 29].

Despite this progress, the literature still lacks enough equal swept-area experimental evidence under a common electrical interface, so it remains difficult to translate aerodynamic comparisons into delivered electrical power for FNC microloads [23, 26]. Modern performance evaluation increasingly uses multivariate power-curve models and robust data-driven inference to separate the effects of inflow, operating point, and turbine design on measured output, but small-scale experimental comparisons still apply these tools inconsistently [30, 31]. Based on this context, this study addresses a focused problem: which compact VAWT rotor provides more usable electrical power per installed swept area for FNC-oriented microloads under the same generator interface and comparable operating conditions?

We test two hypotheses grounded in current VAWT understanding and recent modeling practice: the H-type Darrieus rotor produces higher delivered electrical power and wind-to-electric efficiency than the Savonius rotor on an equal swept-area basis, and turbine type explains more variance in efficiency than wind speed and the tested resistive load levels when evaluated with robust multivariate inference [32, 33]. The objectives of this article are threefold: we quantify delivered electrical power and wind-to-electric efficiency for equal swept-area Savonius and H-type Darrieus rotors under a shared generator interface; we attribute efficiency differences using robust multivariate modeling; and we translate the results into rotor-selection evidence and early-stage sizing inputs for FNC-oriented hybrid systems.

To test these hypotheses, we experimentally compare compact Savonius and H-type Darrieus turbines with identical swept areas (0.45 m^2) and a shared direct-current generator interface under controlled laboratory airflow. We quantify delivered electrical power from measured voltage-current pairs across wind speeds of 1.5–8.0 m/s under discrete resistive loads. We compute wind-to-electric efficiency as the ratio of delivered electrical power to available wind power and estimate turbine-type effects using a multivariate model with robust inference, following recent power-curve modeling advances that support reliable attribution under measurement noise and operating variability. This article contributes (i) equal swept-area experimental evidence under a common electrical interface, (ii) a statistically supported rotor-selection result for FNC-relevant wind speeds, and (iii) practical performance inputs that can inform early-stage sizing of hybrid wind-solar-battery systems for aquaculture microloads.

Edelweiss Applied Science and Technology
ISSN: 2576-8484
Vol. 10, No. 4: 112-124, 2026
DOI: 10.55214/2576-8484.v10i4.12562

2. Method

2.1. Turbine Design and Testing System

This study evaluated two small vertical-axis wind turbine prototypes: a Savonius rotor and an H-type Darrieus rotor designed for application in floating net cages in coastal areas. Both turbines used a rotor diameter of approximately 0.9 m and a rotor height of 0.5 m, which yields the same swept area (0.45 m^2) and enables a fair comparison. The Savonius turbine used three semi-cylindrical blades arranged in a three-stage configuration to prioritize starting torque at low wind speed. The Darrieus turbine used three symmetrical blades in an H-type configuration to exploit lift-driven operation at moderate wind speed. Both rotors were coupled to the same permanent-magnet DC generator through the same shaft and bearing mount to keep drivetrain losses comparable.

The design of the wind turbine model utilized in the study is distinctly illustrated in Figure 1.

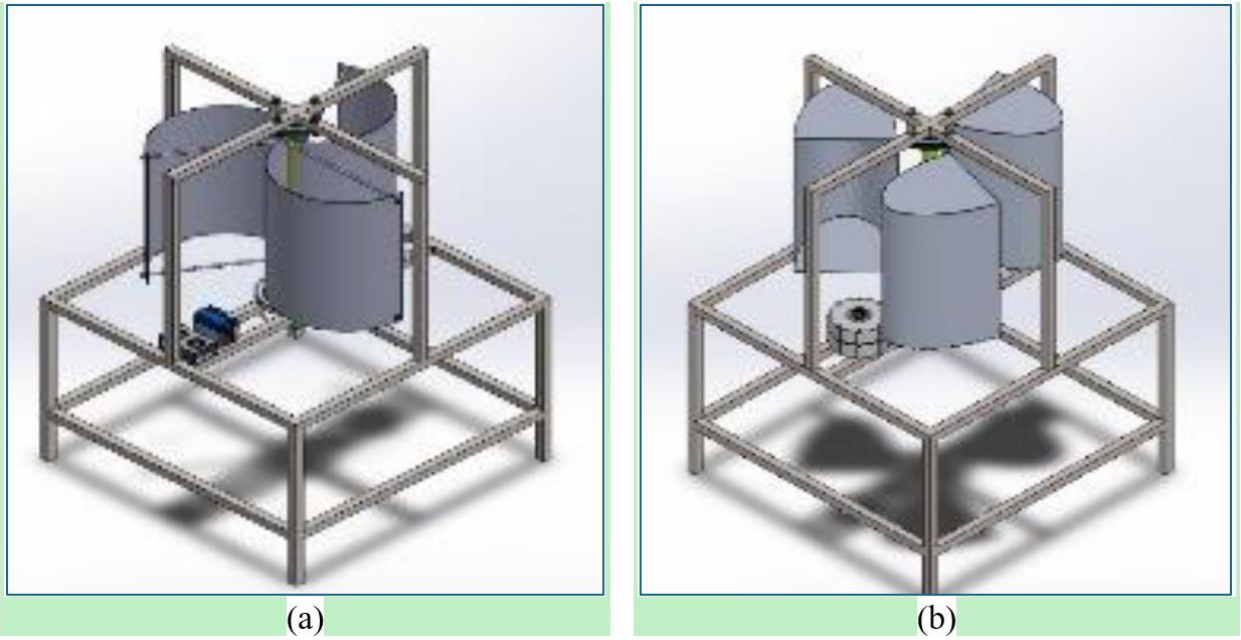

Figure 1.
Wind turbine test prototypes: (a) Savonius, (b) H-type Darrieus.

Experiments were performed in a controlled laboratory environment focusing on electrical machinery, utilizing a device that regulated airflow and demonstrated wind velocities ranging from 1.5 to 8.0 m/s. A digital anemometer was employed to measure the wind speed at the midpoint of the rotor, situated in front of the swept area. A DC multimeter measured output voltage, and output current was measured using a shunt resistor with a multimeter or an equivalent calibrated DC sensor. The generator fed a resistive load bank to emulate low-power floating net cage devices such as LED lighting and small aerators. Load settings ranged from near open circuit to resistance values that drove operation close to the maximum power region. For each combination of turbine type, wind-speed setpoint, and load level, five repeated measurements were recorded to reduce the influence of short-term fluctuations and instrument noise.

2.2. Computation of Electrical Output, Wind Power, and Efficiency

For every logged operating condition, the electrical power produced was calculated using the recorded DC voltage and current measurements [34]:

$$P_{\text{out}} = V \times I \quad (1)$$

Edelweiss Applied Science and Technology
ISSN: 2576-8484
Vol. 10, No. 4: 112-124, 2026
DOI: 10.55214/2576-8484.v10i4.12562

where V_{dc} represents the voltage output in direct current (V), and I_{dc} indicates the current output in direct current (A). The available wind power incident on the rotor, P_{wind}, was calculated using the standard kinetic-energy expression [35]:

$$P_{\text{wind}} = \frac{1}{2}\,\rho\,A\,V_{\text{wind}}^{3} \quad (2)$$

where ρ is air density (kg/m³), A is swept area (m²), and V is mean wind speed (m/s). This study used ρ = 1.225 kg/m³ (sea-level standard) and A = 0.45 m² for both turbines. The conversion efficiency was defined as the ratio of electrical output power to available wind power [36]:

$$\eta = \frac{P_{\text{out}}}{P_{\text{wind}}} \times 100\% \quad (3)$$

All values of P_{out}, P_{wind}, and η were recalculated from the Excel data using Eqs. (1)– (3) to ensure internal consistency and to minimise manual calculation errors.

2.3. Dataset and Descriptive Statistics

The final collection of data comprised 560 operational points, divided equally between the two turbine varieties (280 Savonius and 280 Darrieus). These included incomplete records and clear outliers, such as incorrect readings caused by instrument malfunctions. The wind-speed range spanned from 1.5 to 8.0 m/s, and the load values covered several discrete resistances for each speed level, with five repetitions per wind-speed–load combination. The global descriptive statistics for the two turbine types are summarized in Table 1. Means and standard deviations (SD) were computed for electrical power output and efficiency using all 560 individual data points, and these statistics were used only for global comparison and not as inputs to the regression model.

Table 1.
Summary statistics pertaining to the electrical power output and the total wind-to-electric efficiency for the Darrieus and Savonius turbines.

Turbine type	Mean Electrical Power Output (W)	SD (W)	Mean efficiency (%)	SD (%)
Darrieus	7.59	7.63	17.01	4.74
Savonius	4.47	4.70	10.09	3.19

Table 1 provides the descriptive statistics pertaining to electrical power output and overall wind-to-electric efficiency for the two turbine varieties. To provide a compact summary of how performance changes with wind speed, the study computed mean values at each nominal wind-speed level by aggregating all measurements across load settings and repetitions. Full wind-speed-resolved mean values are provided in Supplementary Table S1 (Appendix A). The Darrieus turbine exhibited a higher average electrical power output compared to the Savonius turbine, recording values of 7.59 W and 4.47 W, respectively. The Darrieus turbine achieved an average efficiency of 17.01%, whereas the Savonius turbine attained an average efficiency of 10.09%. This illustrates a similar pattern concerning the efficiency of the systems analyzed. The Darrieus turbine displayed a more significant variation in its performance outcomes. This suggests that the output experienced greater fluctuations across the different testing methodologies utilized. In conclusion, these results substantiate that the Darrieus turbine achieved a superior average power output compared to the Savonius turbine throughout the particular tests conducted.

For a more focused comparison of turbine performance, Table 2 summarizes the key operating points of electrical power output and overall wind-to-electric efficiency for the Savonius and H-type Darrieus turbines at selected wind speeds.

Edelweiss Applied Science and Technology
ISSN: 2576-8484
Vol. 10, No. 4: 112-124, 2026
DOI: 10.55214/2576-8484.v10i4.12562

Table 2.
Comparison of electrical power output and overall wind-to-electric efficiency between the Savonius and H-type Darrieus turbines at specified wind velocities.

Wind speed (m/s)	n (per turbine)	Mean Electrical power output, H-type Darrieus (W)	Mean efficiency H-type Darrieus (%)	Mean Electrical power output, Savonius (W)	Mean efficiency Savonius (%)	ΔPower (W)	Δη (percentage points)
1.5	20	0.15	16.00	0.10	10.45	0.05	5.55
3.0	20	1.22	16.45	0.80	10.76	0.42	5.69
5.0	20	5.99	17.40	3.47	10.07	2.52	7.33
6.5	20	13.50	17.83	6.89	9.11	6.61	8.72
8.0	20	22.01	15.60	12.47	8.84	9.54	6.76
Overall mean ± SD	280	7.59 ± 7.63	17.01 ± 4.74	4.47 ± 4.70	10.09 ± 3.19	3.12	6.92

Refer to Table 2. The H-type Darrieus turbine consistently outperformed the Savonius turbine. This was accurate regarding the power it generated and its efficacy across all selected wind speeds. The disparity in power increased as the wind intensified. The power reached 9.54 W at a velocity of 8.0 m/s. The effectiveness remained consistent. The most significant disparity in that area was observed at a speed of 6.5 m/s. The H-type Darrieus turbine generated greater average power and exhibited superior efficiency compared to the Savonius turbine under the experimental conditions.

2.4. Regression Modelling and Statistical Analysis

A multiple linear regression (MLR) model was estimated using efficiency η as the response variable to quantify the effects of wind speed, electrical load, and turbine type [37].

$$\eta = \beta_0 + \beta_1 V + \beta_2 R + \beta_3 \text{Type} + \varepsilon \quad (4)$$

where V is wind speed (m/s), R is loading resistance (Ω), and Type is a turbine-type indicator (0 = Savonius; 1 = Darrieus). Parameters β_0–β_3 were estimated using ordinary least squares (OLS). Inference used the heteroskedasticity-consistent covariance estimator HC3. Model effectiveness was assessed through R^2, adjusted R^2, root mean squared error (RMSE), and mean absolute error (MAE). To check the residual data, we used histograms and Q-Q plots, along with the Shapiro-Wilk test to see if the data is normal. The assessment of multicollinearity occurred through the variance inflation factor (VIF), with a VIF below 5 deemed acceptable. Welch's t-test was applied to compare the average efficiencies across different turbine categories, while a two-way analysis of variance (ANOVA) was performed to analyze the impacts of turbine type and wind-speed category on efficiency.

2.5. Data Processing and Software Implementation

Raw measurements were first recorded in Microsoft Excel and then processed using Python. All derived quantities, including electrical power, wind power, efficiency, and the summary statistics per turbine–speed combination, were calculated by means of custom Python scripts. Multiple linear regression with robust standard errors and analysis of variance were also implemented in Python. All figures in this study, power and efficiency curves with error bars, efficiency boxplots, and the measured-versus-predicted efficiency plot, were generated from the same scripts, ensuring that the numerical values in the tables and plots are internally consistent and fully reproducible.

3. Result and Discussion

3.1. Power and Efficiency Trends with Wind Speed

Figure 2 shows the mean electrical output power versus wind speed for both turbines, using the wind-speed-resolved means summarized in Table 2. Power increases strongly with wind speed for both rotors, consistent with the cubic dependence of available wind power. At every wind-speed level, the H-type Darrieus turbine delivers higher mean power than the Savonius turbine. At 1.5 m/s, both machines

Edelweiss Applied Science and Technology
ISSN: 2576-8484
Vol. 10, No. 4: 112-124, 2026
DOI: 10.55214/2576-8484.v10i4.12562

produce very low power (0.15 W for Darrieus and 0.10 W for Savonius), which indicates limited harvestable energy at very low wind speeds. The Darrieus rotor has a mean power of about 6–10 W at 5.0–6.0 m/s, while the Savonius rotor has a mean power of about 3–6 W. At 8.0 m/s, mean power is 22.01 W for the Darrieus rotor and 12.47 W for the Savonius rotor. These trends align with Table 1, where mean power across all operating points equals 7.59 W (Darrieus) and 4.47 W (Savonius), with standard deviations of 7.62 W and 4.70 W, respectively. This separation is consistent with recent small-scale VAWT studies that report stronger energy yield from lift-driven configurations under comparable operating conditions [38].

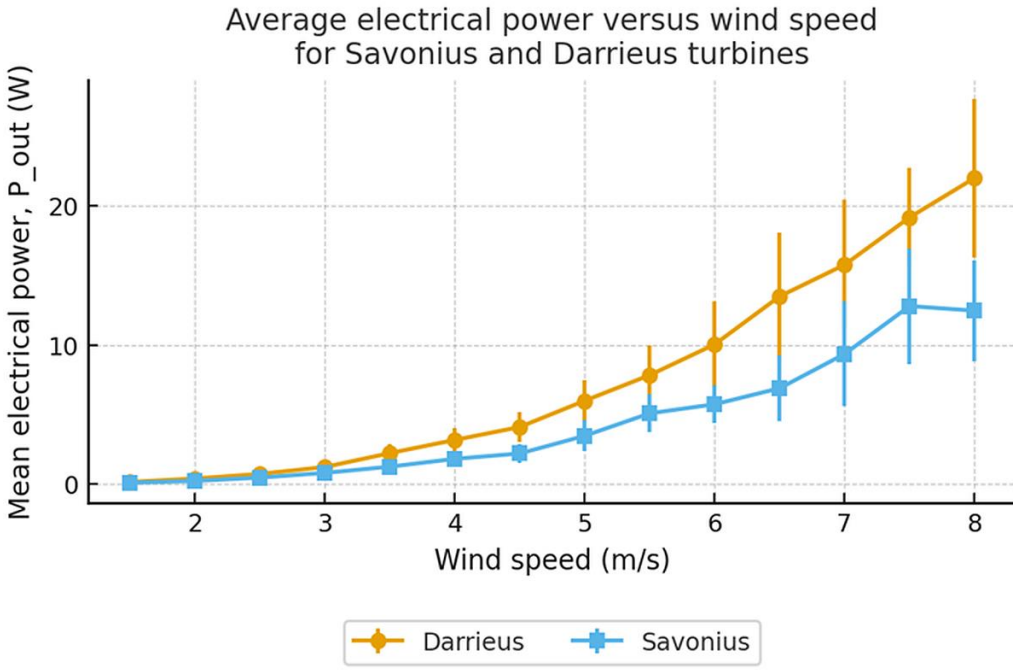

Figure 2.
Average electrical power output at different wind speeds for the Darrieus and Savonius turbines.

Figure 3 presents the mean overall wind-to-electric efficiency at each wind speed level. The Darrieus turbine maintains relatively stable efficiency across most of the tested range: from 1.5 to 7.5 m/s, mean efficiency remains within approximately 16–18%, decreasing slightly to 15.60% at 8.0 m/s. This drop at the highest speed may be due to increased aerodynamic and mechanical losses at higher speeds. The Savonius turbine shows lower efficiency throughout the range, typically between about 9% and 11%, with local dips such as 8.75% at 4.5 m/s and 8.84% at 8.0 m/s. Across all 280 operating points per turbine, the global mean efficiency is 17.01% for the Darrieus rotor and 10.09% for the Savonius rotor (Table 1). The magnitude and direction of this gap align with broader literature that reports higher conversion effectiveness for H-type Darrieus designs than for drag-dominant Savonius rotors when the operating envelope supports lift generation [39].

Edelweiss Applied Science and Technology
ISSN: 2576-8484
Vol. 10, No. 4: 112-124, 2026
DOI: 10.55214/2576-8484.v10i4.12562

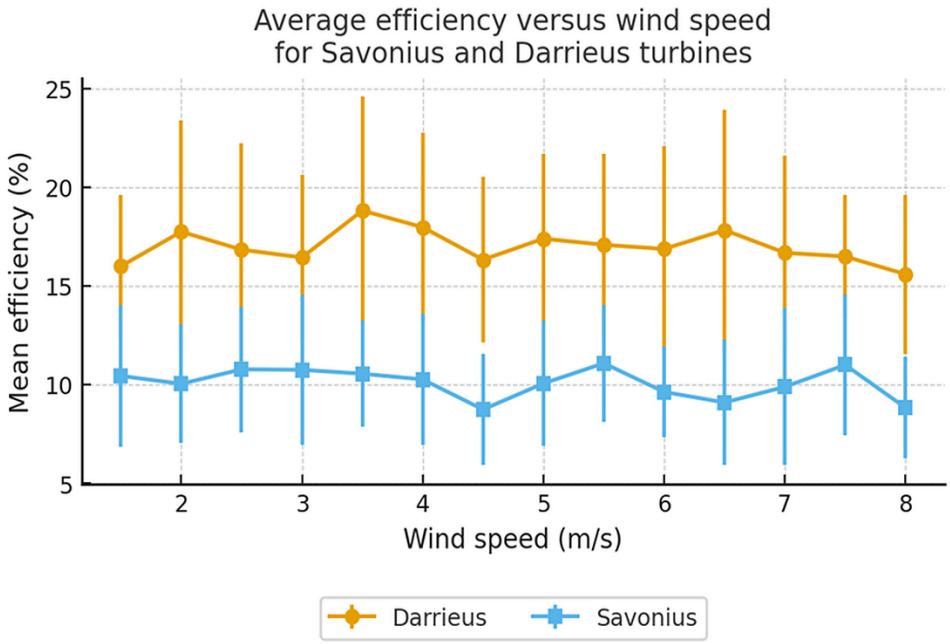

Figure 3.
Average efficiency versus wind speed for the Darrieus and Savonius turbines.

The error bars in Figures 2 and 3 represent ±1 standard deviation around the mean at each wind-speed level, aggregated across all loads and repetitions. They summarize variability due to short-term airflow fluctuations, electrical loading, and measurement noise. The spread is modest relative to the mean trends, which indicates that the observed performance gap is not driven by a small number of extreme measurements. Formal statistical analysis is therefore appropriate for attributing efficiency differences to turbine type and operating conditions, as discussed next. Power and efficiency respond differently to wind speed. Power increases with wind speed because available wind power scales with V^3, but efficiency is normalized by P_{wind}. As a result, wind-speed effects largely cancel in η, so turbine type dominates the efficiency separation in this dataset.

3.2. Regression Model Performance

To analyze the combined influence of wind speed, electrical load, and turbine type on efficiency, a multiple linear regression model was fitted to a full set of 560 operating points, as described in Section 2.4. Efficiency was taken as the response variable, while wind speed, load resistance, and a binary turbine-type indicator (0 for Savonius, 1 for Darrieus) were used as predictors. The model coefficients, derived through ordinary least squares employing robust standard errors (HC3), are presented in Table 3.

Table 3.
Multiple linear regression results for overall wind-to-electric efficiency.

Parameter	Coefficient	Std. error	z-value	p-value
Intercept	10.44	0.51	20.58	< 0.001
Wind speed (m/s)	−0.12	0.08	−1.40	0.16
Load (Ω)	0.03	0.03	0.87	0.39
Turbine type (0/1) *	6.92	0.34	20.21	< 0.001

Note: *0 = Savonius, 1 = Darrieus.

Edelweiss Applied Science and Technology
ISSN: 2576-8484
Vol. 10, No. 4: 112-124, 2026
DOI: 10.55214/2576-8484.v10i4.12562

Table 3 shows that turbine type was the only significant predictor of overall wind-to-electric efficiency. The positive coefficient for turbine type indicates that the H-type Darrieus turbine achieved, on average, 6.92 percentage points higher efficiency than the Savonius turbine after controlling for wind speed and load. In contrast, the variables of wind speed and load did not exhibit statistically significant effects, as indicated by p-values of 0.16 and 0.39, respectively. These findings imply that the efficiency differences observed were predominantly influenced by the type of rotor, rather than variations in wind speed or load levels examined. Table 3 indicates that turbine type was the only significant predictor of overall efficiency. The H-type Darrieus turbine showed a 6.92 percentage-point efficiency advantage over the Savonius turbine, while wind speed and load were not statistically significant.

The model explains a moderate share of the variability in efficiency, with $R^2 = 0.427$ and adjusted $R^2 = 0.424$. The mean absolute error is 3.00 percentage points, and the root mean squared error is 4.02 percentage points. Table 3 shows a strong and highly significant turbine-type coefficient. After adjusting for wind velocity and load resistance, the Darrieus turbine demonstrates an efficiency that surpasses that of the Savonius turbine by 6.92 percentage points ($p < 0.001$). Coefficients for wind speed and load are small and not statistically significant at the 5% level. This outcome aligns with the nearly flat efficiency curves in Figure 3: when efficiency is defined as the ratio between electrical power and available wind power, much of the wind-speed dependence cancels, and remaining variations are small compared with the turbine-type effect.

To evaluate how well the regression model represented the observed efficiency values, the relationship between measured and predicted efficiency is shown in Figure 4.

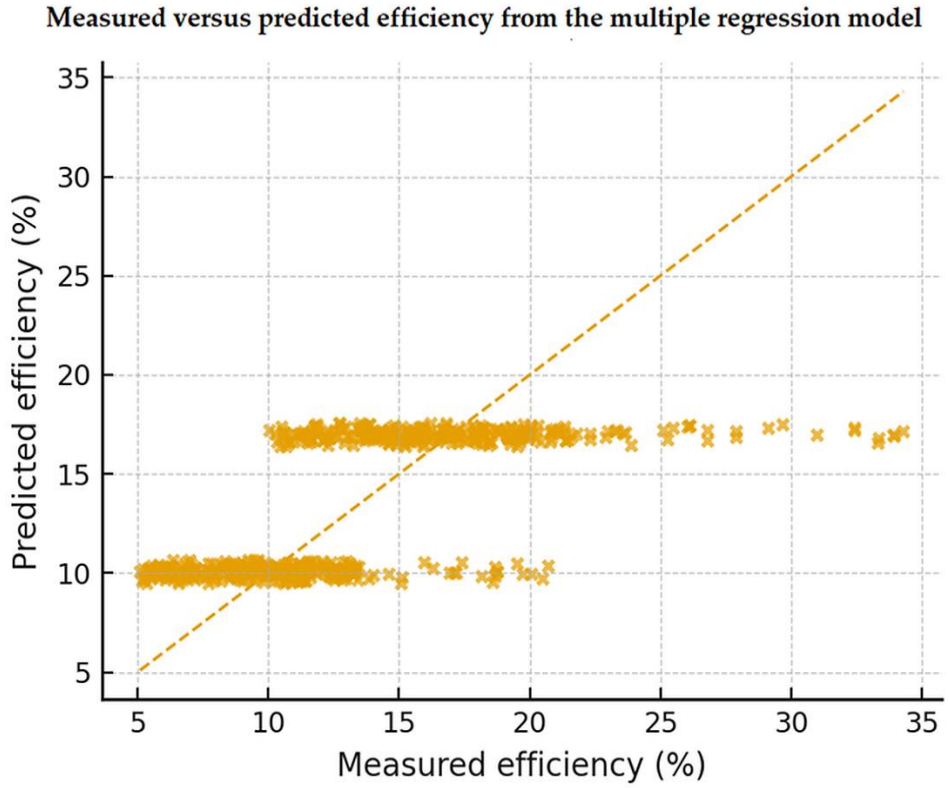

Figure 4.
Measured versus predicted efficiency from the multiple regression model.

Figure 4 shows that most points cluster around the 1:1 line, with a spread consistent with the RMSE and MAE reported above. The absence of strong systematic deviations suggests that the linear

Edelweiss Applied Science and Technology
ISSN: 2576-8484
Vol. 10, No. 4: 112-124, 2026
DOI: 10.55214/2576-8484.v10i4.12562

specification provides an adequate first-order description for this dataset, although more detailed aerodynamic and electromechanical models would be needed to represent all nonlinear effects.

3.3. Comparative Statistical Analysis and Efficiency Distribution

Welch's two-sample t-test compared the 280 Savonius efficiency values with the 280 Darrieus values and yielded $t \approx -20.27$ with $p < 0.001$. Mean efficiency equals 10.09% for the Savonius rotor and 17.01% for the Darrieus rotor, so the mean difference is 6.92 percentage points in favor of the Darrieus configuration. This estimate matches the turbine-type coefficient in Table 3 and confirms that the efficiency separation is not attributable to sampling variability. A two-way ANOVA with turbine type and wind-speed class as factors further indicates a strong main effect of turbine type ($F \approx 407.4$, $p < 0.001$), while wind-speed class is not significant ($F \approx 1.0$, $p \approx 0.47$) and the interaction is not significant ($F \approx 0.66$, $p \approx 0.80$). In order to facilitate a more comprehensive comparison of the overall efficiency characteristics of both turbines at all operating points, the efficiency distribution is illustrated in Figure 5.

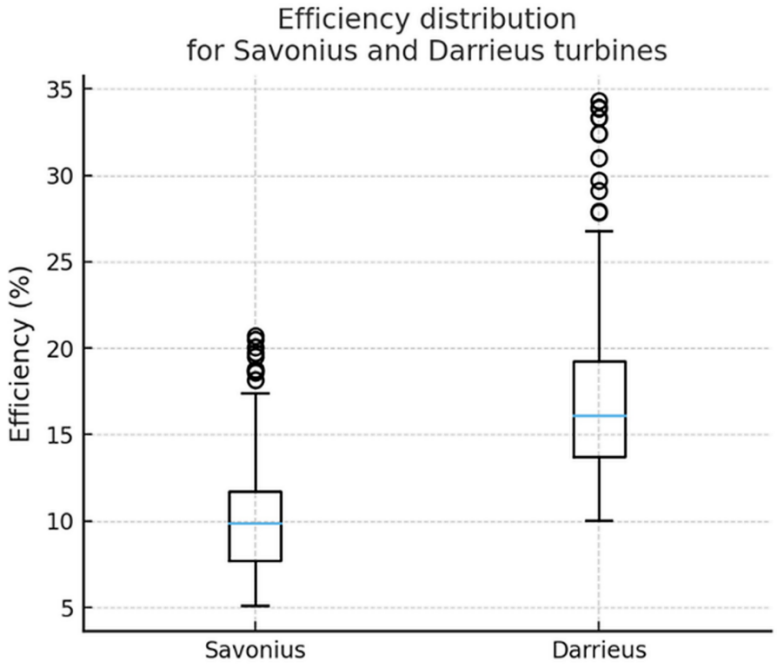

Figure 5.
Distribution of efficiency for Savonius and Darrieus turbines (boxplots derived from all experimental operating points).

The results suggest that the configuration of the rotor serves as the primary factor influencing efficiency within this dataset. The boxplots illustrated in Figure 5 demonstrate that the data for the Darrieus turbine exceeds that of the Savonius turbine, as evidenced by its elevated median and interquartile range. Despite the existence of variations attributed to different loads and multiple trials, the difference between the two distributions is evidently discernible. Collectively, the regression analysis, t-test, and ANOVA yield consistent findings that the H-type Darrieus turbine is more effective in converting available wind power into electrical output than the Savonius rotor under the examined conditions.

Edelweiss Applied Science and Technology
ISSN: 2576-8484
Vol. 10, No. 4: 112-124, 2026
DOI: 10.55214/2576-8484.v10i4.12562

3.4. Implications for Floating Net Cage Applications

The findings examined in this discourse hold significant implications for the electrification of microloads linked to floating net cages. Typical nocturnal requirements encompass low-power LED illumination, diminutive aerators aimed at sustaining dissolved oxygen levels, and sensors for water quality monitoring. During moderate wind velocities, specifically in the range of 5–6 m/s, the Darrieus turbine yields a mean electrical output of approximately 6–10 W, whereas the Savonius rotor generates an estimated 3–6 W under analogous circumstances. At 8.0 m/s, the Darrieus turbine reaches a mean power of about 22 W. Although a single small rotor cannot supply large loads, these results indicate that arrays of small Darrieus turbines can contribute meaningfully to essential low-power services, particularly when integrated with photovoltaic generation and battery storage. The Savonius rotor remains relevant where very low-speed self-starting, mechanical simplicity, and robustness outweigh peak energy yield [40, 41]. Future work should extend the present dataset by adding start-up metrics, testing representative nonlinear loads (drivers and converters), and embedding the resulting performance maps into system-level techno-economic optimization for hybrid wind–solar–battery designs.

4. Conclusion

This study aimed to determine the more suitable small vertical-axis wind turbine rotor for supplying renewable electricity to floating net cages by comparing a Savonius rotor and an H-type Darrieus rotor on an equal swept-area basis and under the same generator interface, using delivered electrical power and wind-to-electric efficiency as performance criteria. The results directly meet this objective: across the tested operating range, the H-type Darrieus turbine consistently produced higher electrical power and a higher mean wind-to-electric efficiency (17.01% versus 10.09%), confirming that, when the design goal is to maximize usable electrical energy per installed swept area for floating net-cage loads, the H-type Darrieus configuration is the preferred rotor within the evaluated envelope. This outcome is consistent with established aerodynamic theory and prior studies showing that lift-driven rotors can achieve higher conversion effectiveness than drag-driven rotors under suitable wind conditions, while also preserving the practical relevance of Savonius turbines for contexts where simplicity and self-starting behavior are prioritized. Robust statistical attribution supports the conclusion by identifying turbine type as the dominant determinant of efficiency (6.92 percentage-point advantage, $p < 0.001$), whereas wind speed and the tested resistive load levels did not significantly shift mean efficiency, which is consistent with the ratio-based efficiency definition that partially cancels wind-speed dependence. Overall, the findings provide evidence-based rotor selection guidance and practical inputs for early-stage sizing of hybrid wind–solar–battery systems for floating net cages, with future work needed to add start-up metrics, non-linear device loads, and battery-charging interfaces for direct field deployment.

Transparency:

The authors confirm that the manuscript is an honest, accurate, and transparent account of the study; that no vital features of the study have been omitted; and that any discrepancies from the study as planned have been explained. This study followed all ethical practices during writing.

Acknowledgements:

This research was funded by the Directorate of Research, Technology and Community Service, Directorate-General of Higher Education, Research and Technology, through the Regular Fundamental Research Grant scheme, contract number: 090/E5/PG.02.00.PL/2024.

References
[1] Q. Jiang, N. Bhattarai, M. Pahlow, and Z. Xu, "Environmental sustainability and footprints of global aquaculture," *Resources, Conservation and Recycling*, vol. 180, p. 106183, 2022. https://doi.org/10.1016/j.resconrec.2022.106183

[2] J. Cao, J. Liu, X. Liu, C. Zeng, H. Hu, and Y. Luo, "A review of marine renewable energy utilization technology and its integration with aquaculture," *Energies*, vol. 18, no. 9, p. 2343, 2025. https://doi.org/10.3390/en18092343

[3] N. T. Nguyen *et al.*, "A comprehensive review of aeration and wastewater treatment," *Aquaculture*, vol. 591, p. 741113, 2024. https://doi.org/10.1016/j.aquaculture.2024.741113

[4] R. Ghamkhar, S. E. Boxman, K. L. Main, Q. Zhang, M. A. Trotz, and A. Hicks, "Life cycle assessment of aquaculture systems: Does burden shifting occur with an increase in production intensity?," *Aquacultural Engineering*, vol. 92, p. 102130, 2021. https://doi.org/10.1016/j.aquaeng.2020.102130

[5] M. Zoli and J. Bacenetti, "Energy analysis in fish aquaculture: Cumulative energy demand of different farming systems," *Aquacultural Engineering*, vol. 110, p. 102525, 2025. https://doi.org/10.1016/j.aquaeng.2025.102525

[6] R. E. Scroggins *et al.*, "Renewable energy in fisheries and aquaculture: Case studies from the United States," *Journal of Cleaner Production*, vol. 376, p. 134153, 2022. https://doi.org/10.1016/j.jclepro.2022.134153

[7] R. Hassan, B. K. Das, and M. Hasan, "Integrated off-grid hybrid renewable energy system optimization based on economic, environmental, and social indicators for sustainable development," *Energy*, vol. 250, p. 123823, 2022. https://doi.org/10.1016/j.energy.2022.123823

[8] R. Zhang, T. Chen, Y. Wang, and M. Short, "Systems approaches for sustainable fisheries: A comprehensive review and future perspectives," *Sustainable Production and Consumption*, vol. 41, pp. 242-252, 2023. https://doi.org/10.1016/j.spc.2023.08.013

[9] Y. Liu *et al.*, "Collaborative water-electricity operation optimization of a photovoltaic/pumped storage-based aquaculture energy system considering water evaporation effects," *Renewable Energy*, vol. 237, p. 121886, 2024. https://doi.org/10.1016/j.renene.2024.121886

[10] N. T. Nguyen, R. Matsuhashi, and T. T. B. C. Vo, "A design on sustainable hybrid energy systems by multi-objective optimization for aquaculture industry," *Renewable Energy*, vol. 163, pp. 1878-1894, 2021. https://doi.org/10.1016/j.renene.2020.10.024

[11] S. Benjamins *et al.*, "Potential environmental impacts of floating solar photovoltaic systems," *Renewable and Sustainable Energy Reviews*, vol. 199, p. 114463, 2024. https://doi.org/10.1016/j.rser.2024.114463

[12] Z. Liu, C. Ma, X. Li, Z. Deng, and Z. Tian, "Aquatic environment impacts of floating photovoltaic and implications for climate change challenges," *Journal of Environmental Management*, vol. 346, p. 118851, 2023. https://doi.org/10.1016/j.jenvman.2023.118851

[13] F. Song, Z. Lu, Z. Guo, Y. Wang, and L. Ma, "The effects of a fishery complementary photovoltaic power plant on the near-surface meteorology and water quality of coastal aquaculture ponds," *Water*, vol. 16, no. 4, p. 526, 2024. https://doi.org/10.3390/w16040526

[14] H. Guo *et al.*, "Global trends and evolution of aquavoltaics in sustainable aquaculture and energy generation," *Renewable Energy*, vol. 255, p. 123864, 2025. https://doi.org/10.1016/j.renene.2025.123864

[15] R. Nobre *et al.*, "Potential ecological impacts of floating photovoltaics on lake biodiversity and ecosystem functioning," *Renewable and Sustainable Energy Reviews*, vol. 188, p. 113852, 2023. https://doi.org/10.1016/j.rser.2023.113852

[16] R. I. Woolway, G. Zhao, S. M. G. Rocha, S. J. Thackeray, and A. Armstrong, "Decarbonization potential of floating solar photovoltaics on lakes worldwide," *Nature Water*, vol. 2, no. 6, pp. 566-576, 2024. https://doi.org/10.1038/s44221-024-00251-4

[17] R. L. Nobre *et al.*, "Floating photovoltaics strongly reduce water temperature: A whole-lake experiment," *Journal of Environmental Management*, vol. 375, p. 124230, 2025. https://doi.org/10.1016/j.jenvman.2025.124230

[18] S. Gorjian, H. Sharon, H. Ebadi, K. Kant, F. B. Scavo, and G. M. Tina, "Recent technical advancements, economics and environmental impacts of floating photovoltaic solar energy conversion systems," *Journal of Cleaner Production*, vol. 278, p. 124285, 2021. https://doi.org/10.1016/j.jclepro.2020.124285

[19] A. Huda, I. Kurniawan, K. F. Purba, R. Ichwani, and R. Fionasari, "Techno-economic assessment of residential and farm-based photovoltaic systems," *Renewable Energy*, vol. 222, p. 119886, 2024. https://doi.org/10.1016/j.renene.2023.119886

[20] J. Jurasz, M. Guezgouz, P. E. Campana, and A. Kies, "On the impact of load profile data on the optimization results of off-grid energy systems," *Renewable and Sustainable Energy Reviews*, vol. 159, p. 112199, 2022. https://doi.org/10.1016/j.rser.2022.112199

Edelweiss Applied Science and Technology
ISSN: 2576-8484
Vol. 10, No. 4: 112-124, 2026
DOI: 10.55214/2576-8484.v10i4.12562

[21] M. A. Abdoulaye, S. Waita, C. W. Wekesa, and J. M. Mwabora, "Optimal sizing of an off-grid and grid-connected hybrid photovoltaic-wind system with battery and fuel cell storage system: A techno-economic, environmental, and social assessment," *Applied Energy*, vol. 365, p. 123201, 2024. https://doi.org/10.1016/j.apenergy.2024.123201

[22] M. Shabani, E. Dahlquist, F. Wallin, and J. Yan, "Techno-economic impacts of battery performance models and control strategies on optimal design of a grid-connected PV system," *Energy Conversion and Management*, vol. 245, p. 114617, 2021. https://doi.org/10.1016/j.enconman.2021.114617

[23] S. Li *et al.*, "Experimental investigation of solidity and other characteristics on dual vertical axis wind turbines in an urban environment," *Energy Conversion and Management*, vol. 229, p. 113689, 2021. https://doi.org/10.1016/j.enconman.2020.113689

[24] P. Zhao, Y. Jiang, S. Liu, T. Stoesser, L. Zou, and K. Wang, "Investigation of fundamental mechanism leading to the performance improvement of vertical axis wind turbines by deflector," *Energy Conversion and Management*, vol. 247, p. 114680, 2021. https://doi.org/10.1016/j.enconman.2021.114680

[25] Y. Li, G. Tong, Y. Ma, F. Feng, and K. Tagawa, "Numerical study on aerodynamic performance improvement of the straight-bladed vertical axis wind turbine by using wind concentrators," *Renewable Energy*, vol. 219, p. 119545, 2023. https://doi.org/10.1016/j.renene.2023.119545

[26] W. Xu *et al.*, "High-resolution numerical simulation of the performance of vertical axis wind turbines in urban area: Part I, wind turbines on the side of single building," *Renewable Energy*, vol. 177, pp. 461-474, 2021. https://doi.org/10.1016/j.renene.2021.04.071

[27] M. Sun *et al.*, "A novel small-scale H-type Darrieus vertical axis wind turbine manufactured of carbon fiber reinforced composites," *Renewable Energy*, vol. 238, p. 121923, 2025. https://doi.org/10.1016/j.renene.2024.121923

[28] A. S. Saad, A. Elwardany, I. I. El-Sharkawy, S. Ookawara, and M. Ahmed, "Performance evaluation of a novel vertical axis wind turbine using twisted blades in multi-stage Savonius rotors," *Energy Conversion and Management*, vol. 235, p. 114013, 2021. https://doi.org/10.1016/j.enconman.2021.114013

[29] W. Tian, X. Ni, Z. Mao, and Y.-F. Wang, "Study on the performance of a new VAWT with overlapped side-by-side Savonius rotors," *Energy Conversion and Management*, vol. 264, p. 115746, 2022. https://doi.org/10.1016/j.enconman.2022.115746

[30] D. Karamichailidou, V. Kaloutsa, and A. Alexandridis, "Wind turbine power curve modeling using radial basis function neural networks and tabu search," *Renewable Energy*, vol. 163, pp. 2137-2152, 2021. https://doi.org/10.1016/j.renene.2020.10.020

[31] Y. Qiao, S. Han, Y. Zhang, Y. Liu, and J. Yan, "A multivariable wind turbine power curve modeling method considering segment control differences and short-time self-dependence," *Renewable Energy*, vol. 222, p. 119894, 2024. https://doi.org/10.1016/j.renene.2023.119894

[32] R. Zou, J. Yang, Y. Wang, F. Liu, M. Essaaidi, and D. Srinivasan, "Wind turbine power curve modeling using an asymmetric error characteristic-based loss function and a hybrid intelligent optimizer," *Applied Energy*, vol. 304, p. 117707, 2021. https://doi.org/10.1016/j.apenergy.2021.117707

[33] Y. Pan and J. Qin, "A novel probabilistic modeling framework for wind speed with highlight of extremes under data discrepancy and uncertainty," *Applied Energy*, vol. 326, p. 119938, 2022. https://doi.org/10.1016/j.apenergy.2022.119938

[34] V. Sethi, K. Sumathy, S. Yuvarajan, and D. Pal, "Mathematical model for computing maximum power output of a PV solar module and experimental validation," *Journal of Fundamentals of Renewable Energy and Applications*, vol. 2, no. 2, pp. 1-5, 2012.

[35] A. Kalmikov, *Wind power fundamentals. In T. M. Letcher (Ed.), Wind energy engineering: A handbook for onshore and offshore wind turbines*. London, UK: Academic Press, 2023.

[36] D. V. Samokhvalov and A. I. Jaber, "Estimation of the maximum efficiency and mechanical performance output from wind turbine," presented at the 2019 XXII International Conference on Soft Computing and Measurements (SCM)) (pp. 81-84). IEEE, 2019.

[37] D. Astolfi, F. Castellani, and F. Natili, "Wind turbine multivariate power modeling techniques for control and monitoring purposes," *Journal of Dynamic Systems, Measurement, and Control*, vol. 143, no. 3, p. 034501, 2021. https://doi.org/10.1115/1.4048490

[38] U. K. Patel, N. Alom, and U. K. Saha, "Lift-based offshore vertical-axis wind turbines for power generation: Current status of technology and future direction of numerical research," *Wind Engineering*, vol. 49, no. 3, pp. 782-809, 2025. https://doi.org/10.1177/0309524X241288094

[39] K. Venkatraman, S. Moreau, J. Christophe, and C. Schram, "Numerical investigation of h-Darrieus wind turbine aerodynamics at different tip speed ratios," *International Journal of Numerical Methods for Heat & Fluid Flow*, vol. 33, no. 4, pp. 1489-1512, 2023. https://doi.org/10.1108/HFF-09-2022-0562

[40] N. Kamaruddin and M. S. M. Shamsuddin, "Experimental investigation of the power storage system for savonius turbines in wind and water," *Journal of Advanced Research in Applied Sciences and Engineering Technology*, vol. 28, no. 3, pp. 235-247, 2022. https://doi.org/10.37934/araset.28.3.235247

[41] K. Nachaiyaphum and C. Photong, "An electric power generation improvement for small Savonius wind turbines under low-speed wind," *Indonesian Journal of Electrical Engineering and Computer Science*, vol. 29, no. 2, pp. 618-625, 2023.

Edelweiss Applied Science and Technology
ISSN: 2576-8484
Vol. 10, No. 4: 112-124, 2026
DOI: 10.55214/2576-8484.v10i4.12562

Appendix A.

Supplementary Table S1

Supplementary Table S1. Mean electrical output power and overall wind-to-electric efficiency of the Savonius and H-type Darrieus turbines at each nominal wind speed (1.5–8.0 m/s, 0.5 m/s increments). Values are aggregated across all load settings and repetitions. Δ denotes Darrieus minus Savonius.

Wind speed (m/s)	P_{out} Darrieus (W)	Efficiency Darrieus (%)	P_{out} Savonius (W)	Efficiency Savonius (%)
1.5	0.15	16.00	0.10	10.45
2.0	0.39	17.75	0.22	10.05
2.5	0.73	16.84	0.46	10.78
3.0	1.22	16.45	0.80	10.76
3.5	2.22	18.82	1.25	10.56
4.0	3.17	17.98	1.81	10.27
4.5	4.10	16.33	2.20	8.75
5.0	5.99	17.40	3.47	10.07
5.5	7.83	17.09	5.09	11.09
6.0	10.05	16.88	5.74	9.64
6.5	13.50	17.83	6.89	9.11
7.0	15.77	16.68	9.36	9.90
7.5	19.18	16.49	12.80	11.01
8.0	22.01	15.60	12.47	8.84

Edelweiss Applied Science and Technology
ISSN: 2576-8484
Vol. 10, No. 4: 112-124, 2026
DOI: 10.55214/2576-8484.v10i4.12562